Available online at www.sciencedirect.com

ScienceDirect

Procedia Computer Science 140 (2018) 298–305

Procedia Computer Science

www.elsevier.com/locate/procedia

Complex Adaptive Systems Conference with Theme: Cyber Physical Systems and Deep Learning, CAS 2018, 5 November – 7 November 2018, Chicago, Illinois, USA

Real-Time Classification of Earthquake using Deep Learning

H. Serdar Kuyuk[a]* and Ohno Susumu[a]

[a]*Tohoku University, Japan*

Abstract

Existing Earthquake Early Warning Systems (EEWSs) calculates the location and magnitude of an earthquake using real-time waveforms from seismic stations within a few seconds. Typically, three to six stations are necessary to estimate earthquake parameters. Waiting for primary (P-) wave information from closest stations results in a blind-zone area where the arrival of secondary (S-) wave cannot be provided around the epicenter of an earthquake. If an earthquake occurred under a city center, EEWSs would not work even though each building has a seismic sensor in a smart city in future. Here, we present a methodology to classify earthquake vibrations into near-source or far-source within one second after P-wave detection. This will allow warnings to citizens who are the residence of earthquake epicenter in case of an earthquake very close by. We trained a deep learning Long Short-Term Memory (LSTM) network for sequence-to-label classification. 305 three component accelerations recorded between 2000 and 2018 in Japan are used to train the artificial network by extracting thirteen features of one second of P-wave. The accuracy of the methodology is 98.2%. 54 out of 55 near-source waveforms classified correctly and only 2 of 80 waveforms were misclassified. We tested the LSTM network with 2018 Northern Osaka (M 6.1.) earthquakes in Japan where closest stations are correctly identified with 83.3% accuracy. Therefore, smart cities donated with smart automated shut-on/off machines and sensors will be more resilient against earthquake disaster even EEWSs are not available in the blind zone area in future.

Keywords: Earthquake Early Warning System; Deep Learning; Convulational Neural Network; Long Short-Term Memory

* Corresponding author. Tel.: +81-22-272-2117; fax: +81-22-272-2119.
E-mail address: kuyuk@irides.tohoku.ac.jp

10.1016/j.procs.2018.10.316

Main text

Many earthquake early warning systems such as Japanese Meteorological Agency (JMA) and National Research Institute for Earth Science and Disaster Resilience (NEID) in Japan and Earthquake Alarm Systems (ElarmS) in California, USA can estimate the earthquake source information such as magnitude and location of epicenter accurately a few seconds after the first arrival station records [1, 2]. They use one to three seconds data of P-wave information from at least four stations to forecast the source parameters. Primary (P) waves are the fastest seismic waves travel in earth and reach to the seismic stations first. They are compressional waves and carry information rather than energy. Estimating and processing the P-wave in real time together with telemetry latency, network-based EEWSs waits three seconds to eight seconds before giving emergency alarms. Within this time, secondary/shear (S-) waves, which carry destructive energy and are slower than P-waves, already reaches the surface of the earth and around the epicenter. Consequently, this leads to a blind zone area where there is no earthquake information available [3].

In order to build an early warning system that is more reliable and robust for earthquakes that are very close to the location of interest, it is necessary to recognize earthquakes very fast. If you are far from the epicenter, mostly you will get a warning if there is an EEWS in your region. However, there are cases in which systems does not work as expected [2]. Therefore, the objective of this article is to develop a methodology to classify earthquake acceleration records in seismic stations into near-source and far-source. Near source defined as the stations close to epicenter of earthquake and far-source are defined stations that are far from the epicenter. So that, the method can be used for identifying the earthquake if you are in the blind zone where EEWS does not help or if regional EEWS does not work due to technical infrastructure. Previously, some studies tried to classify near-source versus far-sources in the real-time estimation of fault rupture extent using full earthquake acceleration waveform [4]. Such classifications using Fisher's linear discriminant analysis and Bayesian or wavelet-based methods were using peak ground parameters (peak ground acceleration, velocity etc.) they cannot be used for earthquake early warning purposes [4, 5]. Various pattern recognition techniques are also applied to classify earthquakes and for example quarry blast [6, 7, 8].

For this, past recorded earthquake ground motions are analyzed to predict whether a P-wave ground motion is close to the earthquake epicenter. This classification problem can be stated as follows; given a one-second P-wave data from past earthquake acceleration records, can we distinguish that a real-time recording (or seismic station) is the near- or far-source when a new observation is fed.

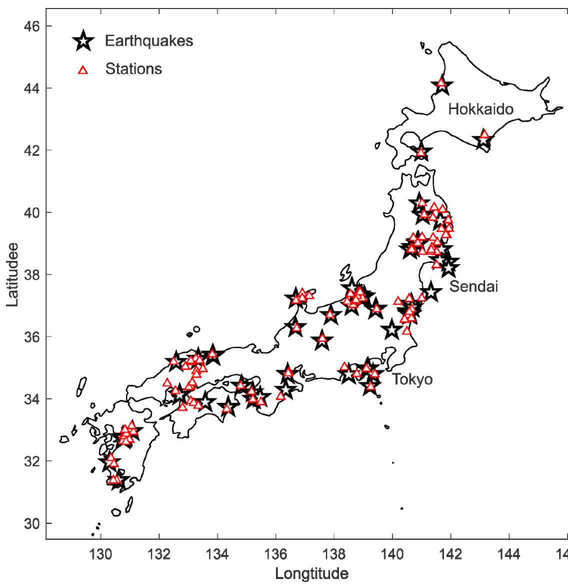

Fig. 1. Map of Japan with earthquakes (black stars) and 55 close stations (red triangles) within 17 epicentral distance.

Existing EEWSs calculate a location and magnitude of an earthquake using real-time waveforms from seismic stations within a few seconds [9]. Typically, P-wave information of three to six stations are necessary to estimate earthquake parameters. Calculations and waiting for three seconds of P-wave information from distant stations results in a blind-zone area where the arrival of secondary (S-) wave cannot be provided around the epicenter of an earthquake. Here, we present a methodology to classify earthquake vibrations into near-source or far-source within one second after P-wave detection. This will allow warnings to citizens who are the residence of earthquake epicenter in case of an earthquake very close by.

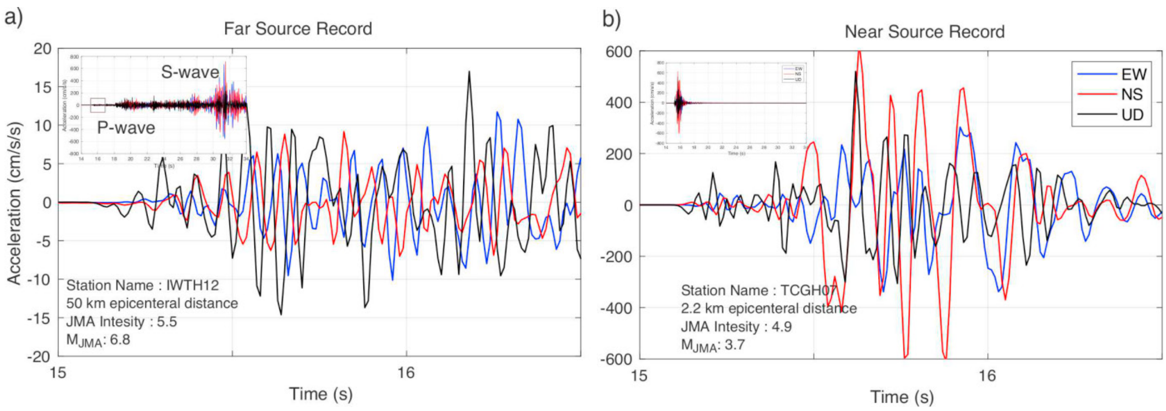

Fig. 2. (a) Far-source recording at IWTH12 stations with 50 km epicentral distance due to 6.8 magnitude earthquake. The small figure shows all records. P-wave and S-wave are distinguishable. First second data goes up to 15 cm/s/s maximum. Different colors indicate east-west, north-south and the up-down component of the record. (b) Near-source recording at TCGH07 station with 2.2 km epicentral distance. First second data contains both P- and S-wave and records with maximum 600 cm/s/s. Small figure at b) shows the duration of the vibration compared to the inner figure in a) with the same time interval.

Strong-Motion Data and Data Sources

We collected strong-motion data from K-NET and KiK-net seismic network archives, operated by NIED, Japan and classify these recordings into two predefined groups; near-source or and far-source records. Those earthquake data is available at the website of seismic networks (http://www.kyoshin.bosai.go.jp/). We have searched near-source earthquakes based on certain selection criteria. The stations with epicentral distance less than 10 km with recorded peak acceleration exceeding 500 cm/s/s are used for this study. 55 earthquakes records are obtained (Fig. 1). These records are from both K-net and Kik-network. Here, we define a near-source station as a station whose hypocenter distance is less than 17 km. Researchers found that the minimum blind zone radius is about 17 km [3]. We have searched far-source records between 17 and 50 km with the same peak ground acceleration exceeding 500 cm/s/s. The reason we applied a threshold of 500 cm/s/s peak ground acceleration is because we want to concentrate earthquakes that create large intensities.

The recordings were various length with standard 100 sample per seconds. Three component waveforms, east-west, north-south, up-down are first filtered by Japanese Meteorological Agency intensity calculations. Then we manually pick the onset of P-waves for a total of 405 recordings. Out of 405 three component strong motion data, 45% (55 stations) are from near-source stations. All waveforms are preprocessed by applying instrument correction (frequency-dependent instrument response), baseline corrections (DC offset), and band-pass filtering. An example of two recordings one in near source and the other in the far-source are shown in Fig. 2.

The first six basic features (time series) extracted from one second of P-wave (100 data points) are three raw EW, NS and UD component and their filtered time series (Figure 3-a,b,c,d,e,f). The next six features are the absolute values and the cumulative sum of absolute values of three components (Figure 3-g,h,i,j,k,l). Then we added the square root of the sum of the squares of the three recordings which shows the geometrical mean of the waveforms. Length of the time series are all same 100 time points. Therefore the size of the input matrix for each station is 13x100.

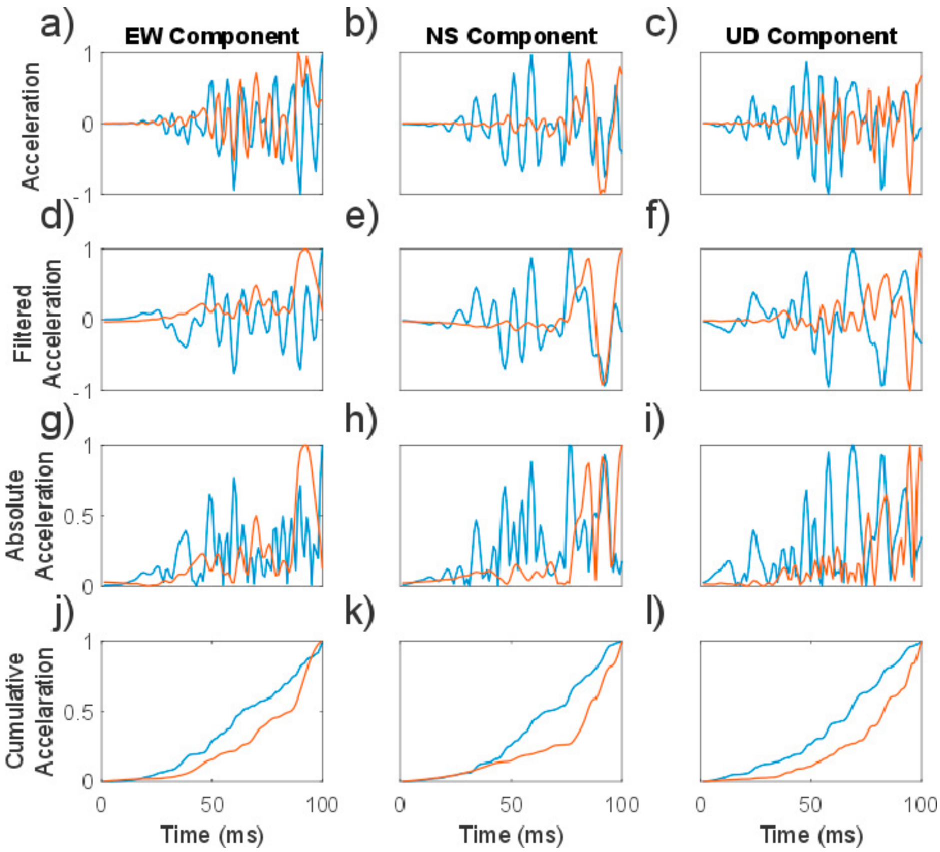

Fig. 3. (a)-(b)-(c) Normalized acceleration records for three component where red line show near-source and blue line shows far source recordings of one-second data. (d)-(e)-(f) are the filtered waveforms shown in upper figures. (g)-(h)-(i) Absolute values of the records. (j)-(k)-(l) Cumulative absolute acceleration records. All data are normalized to the maximum value of one-second data.

The reason we added the absolute and the cumulative sum is due to the difference of amplitude levels of near and far source ground motion. In near-source high-frequency vibration is dominant. This phenomenon is studied by engineers and seismologist. High-frequency ground motion decrease in amplitude more rapidly with distance than low-frequency vibration [10]. Hence, high-frequency motions correlate with epicentral distance better and could be a good measure to classify near- and far-source stations [4].

Methodology

We investigated the applicability of a recurrent, deep-learning Long Short-term Memory Networks (LSTM) algorithm as a discriminant function. Shallow networks such as artificial neural networks are applied to EEWS for different purposes [11, 12, 13]. LSTM is not applied to EEWS but is widely used sentiment analysis, language modeling, speech recognition and video analysis. It is a type of recurrent neural network. They manage learning, processing and classifying sequential data. We have applied LSTM to classify earthquake waveforms which are a sequence of data like speech.

We trained an LSTM network to recognize the near-, far- source earthquake with given one seconds of P wave time series. One second of the waveform is input as a sequence data and made predictions based on each time steps of the waveform. We evaluated 13 features of a convolutional neural network (CNN) to classify waveforms. The network learns these features during training. Time series of features are visualized in Fig. 3 and Fig.4.

In Figure 3, normalized acceleration records for three component where red lines show near-source and blue lines shows far source recordings of one-second data are shown. All data are normalized to the maximum value of one-second data. By looking only the shape of the time-series, there are a few differences and it is hard to distinguish one from another. However near source motion of earthquake is stronger than the far site motion. Ground motion attenuate with distance. This can be seen in Figure 4. Red line (near-source) amplitude is much larger than the blue lines (far source). Figures shows that P-wave is amplitude dependent this is one of the strongest feature that is used in the CNN.

During training, data split into mini-batches and pads the sequences. We have used 40 as mini-batch size so that the training data divided evenly and this reduces the amount of padding in the mini-batches.

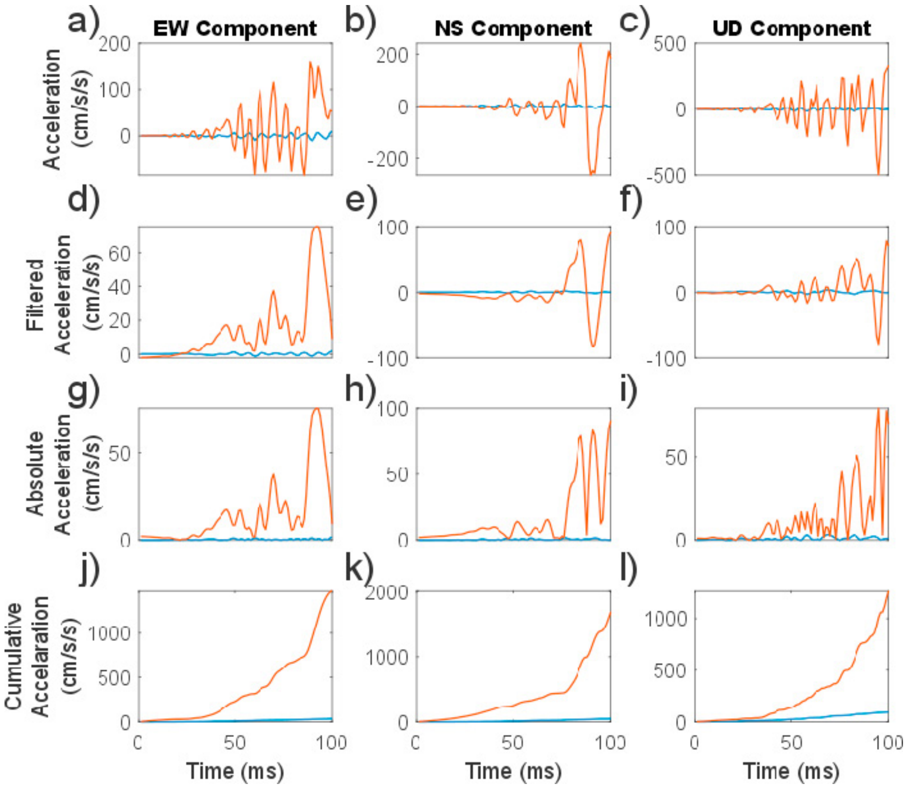

Fig. 4. Same figure with Fig. 3 except values are not normalized and shows actual acceleration values. (a)-(b)-(c) acceleration records for three component where red line show near-source and the blue line shows far source recordings of one-second data. (d)-(e)-(f) are the filtered waveforms shown in upper figures. (g)-(h)-(i) Absolute values of the records. (j)-(k)-(l) Cumulative absolute acceleration records.

Therefore, the input size to be sequences of size is 13. We specified the LSTM layer with 100 hidden units correspond to 100 sample per seconds and the last value is selected as the last element of the sequence. We provided two classes by including a fully connected layer of size two, followed by a softmax layer and a classification layer respectively. The model is developed using MATLAB Neural Network Toolbox.

Results

In the training dataset, there are 55-near, 80-far source station records. Only one record is not labeled near source out of 55 data. The accuracy is 98.2%. Whereas two records are misclassified for the far-source. The accuracy is 97.5%. Totally only 3 out of 135 records are incorrectly labeled (Fig. 5). When we trained the dataset with different options such as changing the learning rate etc., almost similar results are obtained. Therefore the accuracy is saturated at this rate. This shows that the optimization is reached the minimum.

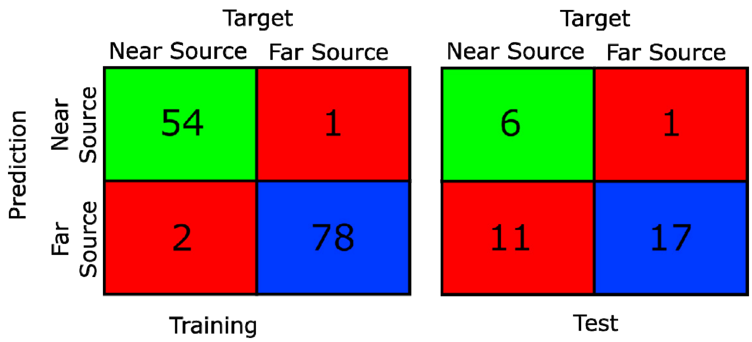

Fig. 5. Performance of convolutional artificial network on training and testing data. The accuracy of training is 98.2% and 65.7% for testing

As for the testing the trained network, we used an actual earthquake records which is not used in the training dataset. In 2018 June,16 an earthquake occurred in the morning in Osaka city center, Japan. Osaka is one of the largest cities in Japan with about 2.7 million residents. This earthquake with magnitude 6.1 killed four people and injured more than 400 people. Recorded maximum JMA intensity in the metropolitan area is 6 minus. This earthquake is very important because of well recorded in the city center with a shallow depth of 13 km.

JMA earthquake early warning system worked nicely and issued an alarm 3.2 seconds after the first vibration received from the closest seismic station. At the time of warning, depth is predicted 10 km and magnitude is 6.0. Results were recognized satisfactorily but there is one issue that, the blind zone is about 23 km from the epicenter (Fig. 6). This means the residents around the epicenter where most potential damage is expected could not be received a warning. This is the one big downside of EEWS that system needs about 3 seconds of records to calculate the size of the earthquake which leads to delays in issuing an alarm.

We have downloaded the closest 35 records of Osaka earthquake (within the 50 km epicentral distance) and tested trained convolution network. There are 7 near- and 28 far- source records in the dataset. Only one station is misclassified in near-source stations. 11 out of 28 is misclassified for the far source records. Total accuracy is 65.7%. 83.3% of near source waveforms are categorized correctly (Fig. 5).

The accuracy drops to 65.7% for far-source stations indicated in red circles in Fig. 6b. The gray dashed line around the epicenter (black star in Fig. 6b) shows the blind zone area. From that point forward the residents of EEWS users get warning seconds to a few ten seconds depending on the distance from the epicenter. The far, the more seconds or warning they get. Although the intensity decrease by the distance. The errors or misclassified stations out of blind zone area is acceptable in terms of warning because the national JMA EEWS already issues magnitude and location of the earthquake with acceptable accuracy.

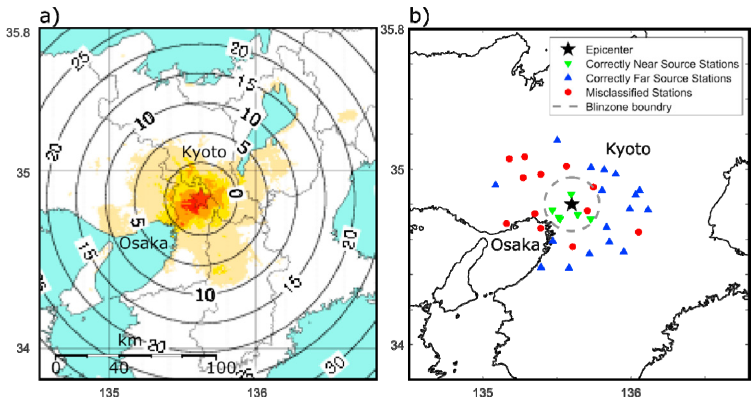

Fig. 6. (a) JMA EEWS report for 2018 Osaka earthquake with M6.1 Circles shows the seconds that are available before S-wave reaches. Yellow to red colors indicate the intensity distribution. Figure is changed from JMA EEWS website [14]. (b) classified near- and far source stations of the CNN

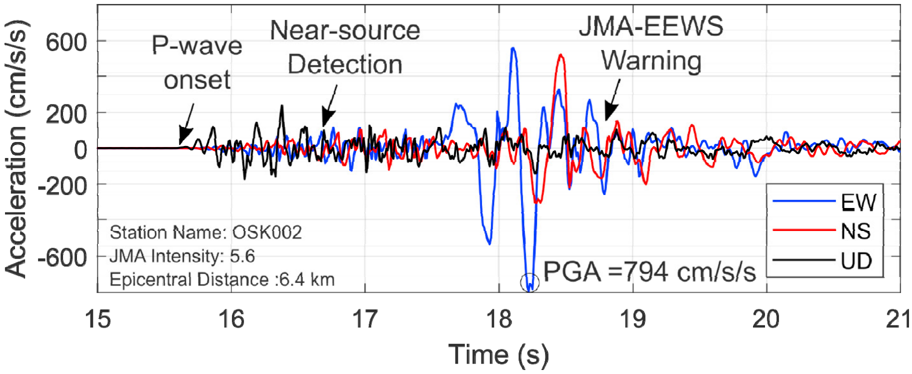

Fig. 7. Three component acceleration records at OSK002 station.

We think if the proposed methodology is implemented into any EEWS, with using the identified near-source stations in one second, there could be an automatic warning even before strong shaking stroke the epicenter. For Osaka earthquake, the closest station OSK002 acceleration record of three component is shown in Fig. 7. P-wave onset starts at 15.6 seconds. One second later near-source algorithm detects the near source earthquake and JMA warning is issued at 18.8 seconds. JMA warning, unfortunately, arrives after peak ground acceleration (PGA) reach the station with 784 cm/s/s. If we add one second of transmission latency, still there could be an automated warning issued before PGA. Latencies generally little than one second in EEWSs [2].

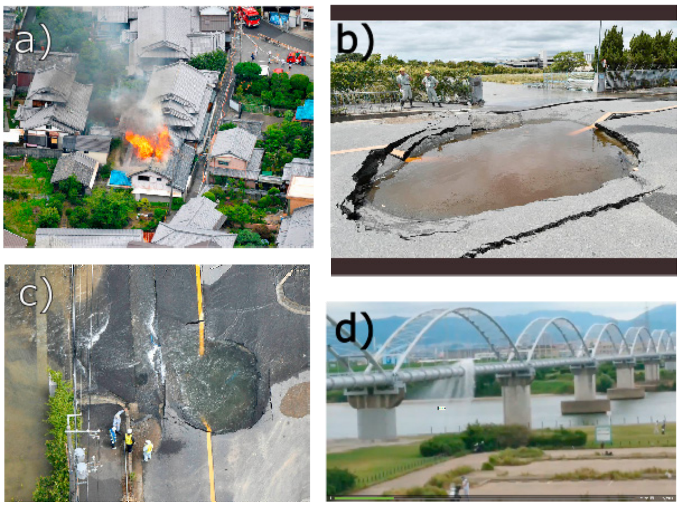

Fig. 8. Various disaster occurred after 2018 Osaka Earthquake. (a) one of the fire break out at a house (b) water fills in the road after water pipes burst (c) flooded road (d) Water gushes from a water infrastructure bridge, (picture (a), (b), (c) obtained from [15], (d) obtained from [16])

These one-two seconds obviously is not sufficient for the human response but adequate for machine response. In Fig. 8, there are couple of disasters happened during the earthquake. There are many fire breakouts and flooded areas due to the failure of the water pipe infrastructure. If there would be automated shutdown valves in the infrastructure nodes, these type of disaster would not happen. Because valves will be shut down within a millisecond. This will allow fixing the cracks easily by civil engineers. This is just one example but applications could be extended to various field such as bridge control or telecom backbone design [17, 18, 19, 20].

Acknowledgments

We have used K-NET and/or KiK-net data from the website of http://www.kyoshin.bosai.go.jp/. The first author thanks to Prof. Dr. Masato Motosaka from Tohoku University, Japan, for his support.

References

[1] Hoshiba, M., Kamigaichi, O., Saito, M., Tsukada, S. Y., and Hamada, N. (2008). “Earthquake early warning starts nationwide in Japan.” *EOS, Transactions American geophysical union*, **89(8)**: 73-74.

[2] Kuyuk H. Serdar, Allen, R. M., Brown, H., Hellweg, M., Henson, I., and Neuhauser, D. (2013). “Designing a network□based earthquake early warning algorithm for California: ElarmS□2.” *Bulletin of the Seismological Society of America*, **104(1)**:162-173.

[3] Kuyuk, H. Serdar, and Allen, R. M. (2013). “Optimal seismic network density for earthquake early warning: A case study from California.” *Seismological Research Letters*, **84(6)**: 946-954.

[4] Yamada, M., Heaton, T., and Beck, J. (2007). “Real-time estimation of fault rupture extent using near-source versus far-source classification.” *Bulletin of the Seismological Society of America*, **97(6)**: 1890-1910.

[5] Kuyuk, H.Serdar, Kuyuk R.Talha, E., Yildirim, Y., Sumer, (2011), “Assessment of Near- And Far- Field Earthquake Ground Motion with Wavelet Transform” *Engineering Sciences*, **6(1)**:

[6] Kuyuk, H. S., E. Yildirim, E. Dogan, and G. Horasan. (2011). "An unsupervised learning algorithm: application to the discrimination of seismic events and quarry blasts in the vicinity of Istanbul." *Natural Hazards and Earth System Sciences*, **11(1)** : 93-100.

[7] Kuyuk, H. Serdar, Eray Yildirim, Emrah Dogan, and Gunduz Horasan. (2014). "Clustering seismic activities using linear and nonlinear discriminant analysis." *Journal of earth science* **25(1)**: 140-145.

[8] Kuyuk, H. S., E. Yildirim, E. Dogan, and G. Horasan. (2012). "Application of k-means and Gaussian mixture model for classification of seismic activities in Istanbul." *Nonlinear Processes in Geophysics* **19(4)**: 411-419.

[9] Kuyuk, H. Serdar, and Richard M. Allen. (2013). "A global approach to provide magnitude estimates for earthquake early warning alerts." *Geophysical Research Letters,* **40(24)**: 6329-6333.

[10] Hanks, Thomas C., and Robin K. McGuire. (1981). "The character of high-frequency strong ground motion.". *Bulletin of the Seismological Society of America*, **71(6)**: 2071-2095.

[11] Kuyuk, H. Serdar. and M. Motosaka, (2009), “Real-Time Ground Motion Forecasting Using Front-Site Waveform Data based on Artificial Neural Network” *Journal of Disaster Research*, **4(4)**:

[12] Böse, Maren, Friedemann Wenzel, and Mustafa Erdik. (2008) "PreSEIS: A neural network-based approach to earthquake early warning for finite faults." *Bulletin of the Seismological Society of America*, **98(1)**: 366-382.

[13] Kuyuk, H.S. and M. Motosaka, (2009), "Forward Spectral Forecasting of Ground Motion with the Information of Earthquake Early Warning Systems for Structural Control" *Journal of Japan Association for Earthquake Engineering*, **9(3)**:

[14] JMA EEWS, (2018) https://www.data.jma.go.jp/svd/eew/data/nc/pub_hist/2018/06/20180618075838/reachtime/reachtime.html

[15] Reuters, https://www.express.co.uk/news/world/975787/Japan-earthquake-Osaka-latest-news-pictures-Takatsuki-damage

[16] Storyfulweather, https://rumble.com/v5ovs3-water-gushes-from-damaged-main-after-japanese-earthquake.html

[17] Kuyuk H.Serdar., Aktas M., Arslan H, (2015). "Bosporus Bridge Traffic Operation Techniques Using Real-time Earthquake Information to Mitigate the Risk Involved", *Disaster Science and Engineering*, **1(1)**, 17-24

[18] Oguz, Melike, Ferhat Dikbiyik, and H. Serdar Kuyuk. (2016). "Earthquake preparedness strategies for telecom backbone with integration of early warning systems and optical WDM networks." *In Resilient Networks Design and Modeling (RNDM), 2016 8th International Workshop on*, 181-188. IEEE.

[19] Kuyuk, H. Serdar, S. Colombelli, A. Zollo, R. M. Allen, and M. O. Erdik. (2015). "Automatic earthquake confirmation for early warning system." *Geophysical Research Letters,* **42(13)**: 5266-5273.

[20] Böse, M., R. Allen, H. Brown, G. Gua, M. Fischer, E. Hauksson, T. Heaten et al. (2014). "CISN ShakeAlert: An earthquake early warning demonstration system for California." *In Early warning for geological disasters*, 49-69. Springer, Berlin, Heidelberg.